



Published in final edited form as:

Am J Med Genet A. 2017 December ; 173(12): 3231–3237. doi:10.1002/ajmg.a.38376.

Defective ciliogenesis in *INPP5E*-related Joubert syndrome

Isabel Hardee^{1,*}, Ariane Soldatos^{1,✉,*}, Mariska Davids^{1,*}, Thierry Vilboux^{2,3}, Camilo Toro⁴, Karen L. David⁵, Carlos R. Ferreira⁴, Michele Nehrebecky⁴, Joseph Snow⁶, Audrey Thurm⁶, Theo Heller⁸, Ellen F. Macnamara¹, Meral Gunay-Aygun^{2,4,9}, Wadih M. Zein⁷, William Gahl^{1,2,4}, and May Christine V. Malicdan^{1,2,4,✉}

¹NIH Undiagnosed Diseases Program, Common Fund, National Human Genome Research Institute, National Institutes of Health, Bethesda, MD

²Medical Genetics Branch, National Human Genome Research Institute, National Institutes of Health, Bethesda, MD

³Department of Medical Genetics, Inova Translational Medicine Institute, Falls Church, VA

⁴Office of the Clinical Director, National Human Genome Research Institute, National Institutes of Health

⁵New York Methodist Hospital, Brooklyn, NY

⁶Office of the Clinical Director, National Institute of Mental Health, National Institutes of Health, Bethesda, MD

⁷Ophthalmic Genetics & Visual Function Branch, National Eye Institute, National Institutes of Health, Bethesda, MD

⁸National Institute of Diabetes and Digestive and Kidney Diseases, NIH, Bethesda, MD

⁹Johns Hopkins University School of Medicine, Department of Pediatrics and McKusick-Nathans Institute of Genetic Medicine, Baltimore, MD 21287, USA

Abstract

Joubert Syndrome is a neurodevelopmental disorder, characterized by malformation of the mid and hindbrain leading to the pathognomonic molar tooth appearance of the brainstem and cerebellum on axial MRI. Core clinical manifestations include hypotonia, tachypnea/apnea, ataxia, ocular motor apraxia, and developmental delay of varying degrees. In addition, a subset of patients has retinal dystrophy, chorioretinal colobomas, hepatorenal fibrocystic disease and polydactyly. Joubert Syndrome exhibits genetic heterogeneity, with mutations identified in more than thirty

✉ Corresponding author: Ariane Soldatos, MD, MPH, ariane.soldatos@nih.gov, phone: 301-496-1562, May Christine V. Malicdan, MD PhD, malicdanm@mail.nih.gov, phone: 301-451-4665.

*These authors contributed equally

Web resources:

ExAC Browser, <http://exac.broadinstitute.org/>, accessed November 9, 2016

Miami ROH tool, http://www.ccs.miami.edu/cgi-bin/ROH/ROH_analysis_tool.cgi

Mutation Taster: <http://www.mutationtaster.org/>

PolyPhen-2, <http://genetics.bwh.harvard.edu/pph2/>

SIFT, <http://sift.bii.a-star.edu.sg/>

genes, including *INPP5E*, a gene encoding inositol polyphosphate 5-phosphatase E, which is important in the development and stability of the primary cilium.

Here we report the detailed clinical phenotypes of two sisters with a novel homozygous variant in *INPP5E* (NM_019892.4: c.1565G>C, NP_063945.2: p.Gly552Ala), expanding the phenotype associated with Joubert Syndrome type 1. Expression studies using patient-derived fibroblasts showed changes in mRNA and protein levels. Analysis of fibroblasts from patients revealed that a significant number of cells had shorter or no cilia, indicating defects in ciliogenesis and cilia maintenance.

Keywords

ciliopathy; molar-tooth sign; rare disorders; Joubert syndrome; INPP5E

INTRODUCTION

Joubert Syndrome (JS) is an autosomal recessive disorder caused by mutations in at least 30 genes that code for proteins in the cilia or centrosome; hence, JS is considered a ciliopathy [Travaglini et al., 2013]. The incidence of JS is estimated at 1 in 80,000-100,000, but this may be an underestimate due to the heterogeneity of the disorder [Brancati et al., 2010] and overlap with other phenotypes such as isolated nephronophthisis, and Senior-Loken syndrome [Malicdan et al., 2015; Travaglini et al., 2013].

The neuroradiological hallmark of JS is the so called “molar tooth sign” (MTS) on axial brain MRI, which results from a specific constellation of mid and hindbrain malformations including cerebellar vermis hypoplasia, thick and abnormally oriented superior cerebellar peduncles, and unusually deep interpeduncular fossa. The finding of the MTS has been noted in prenatal imaging as early as 14–16 weeks of gestation, and considered to be associated with defective decussation of the superior cerebellar peduncles [Doherty 2009].

Over the past several years, an increasing number of genes have been associated with Joubert syndrome, including *INPP5E*, which encodes 1,4,5-triphosphate (InsP3) 5-phosphatase, a 72 kDa protein that hydrolyzes the 5-phosphate of phosphatidylinositol 3,4,5-triphosphate and phosphatidylinositol 4,5-diphosphate. *INPP5E* is concentrated in the axoneme of the primary cilium, and deregulation can alter cilia stability. Primary cilia are antenna-like structures that project from the surfaces of differentiated cells, participating in extracellular signal processing. Previous studies have shown that *INPP5E* plays a critical role in cilia by controlling ciliary growth and phosphoinositide 3-kinase (PI3K) signaling and stability [Jacoby et al., 2009]; no defect in ciliogenesis, however, has been shown in cultured cells from patients. Herein we present detailed clinical phenotyping of two siblings with JS due to novel homozygous mutation in *INPP5E*, and document that patient’s fibroblasts have shorter than normal cilia providing evidence for role of *INPP5E* in cilia formation.

MATERIALS AND METHODS

The patients were admitted to the National Institutes of Health Clinical Center (NIH-CC) and enrolled in protocol 76-HG-0238, “Diagnosis and Treatment of Patients with Inborn Errors of Metabolism or Other Genetic Disorders,” approved by the National Human Genome Research Institute (NHGRI) Institutional Review Board (IRB). After parents gave written informed consent and the patients gave assent, the two sisters at ages 19 years (Patient 1) and 18 years (Patient 2) underwent a 5-day clinical evaluation. Other methods are detailed in Supplementary Information.

RESULTS

Clinical report

Patients 1 and 2 (Figure 1A) are Hispanic sisters who were evaluated twice at the NIH-CC, first for a one-week comprehensive phenotyping visit and then one year later for completion of clinical testing and genetic counseling. Of note, the family is bilingual (English and Mexican) and hence all evaluations were conducted with the assistance of a Spanish interpreter.

The proband (Patient 1) was 19 years of age at initial evaluation. Perinatal history was uneventful; by 2 years of age she had no spoken words but hearing was normal. She was hypotonic and had delayed motor development; she first walked at 3.5 years of age. At school, she was placed in a special education setting because of a full scale IQ of 77. At age 19, she was able to vocalize approximately 10 single words and indicated her needs by pointing and using signs, although she was able to write names and numbers. She was independent in her activities of daily living. For instance, she took the city bus to school by herself and held a part-time job cleaning tables at a mall food court. There were no behavioral concerns. Upon examination, her head circumference was 58 cm (>99th centile, +3SD), height was 154.4 cm (9th centile), and weight was 67 kg (72nd centile). She had some facial dysmorphisms including high-arched eyebrows, small earlobes, and mild prognathism. Her neurological examination was notable for dysarthria, paucity of speech, mild dysmetria, and a mildly wide-based gait. Brain MRI revealed the characteristic MTS (Figure 1B, left panel). Lumbar puncture was notable only for low CSF protein with a value of 8 mg/dL.

Her auditory brainstem response was abnormal bilaterally, consistent with dysfunction of the auditory brainstem pathways. Ophthalmology examination showed bilateral ptosis (right greater than left), rotatory nystagmus, ocular motor apraxia, myopic astigmatism and retinal degeneration with optic nerve drusen (Figure 1B, middle and right panels). Best-corrected visual acuity (BCVA) stood at 0.30 logMAR in each eye. Fundus examination showed evidence of retinal dystrophy and electroretinography (ERG) revealed reduced and delayed photopic responses at around 50% of the lower limit for normal and borderline scotopic responses, consistent with cone-rod dystrophy. On a smell test with the UPSIT, she scored 19/40 consistent with severe microsomia. On neuropsychological evaluation at the NIH, her performance on tests of processing speed, non-verbal reasoning, working memory (mental arithmetic), and receptive vocabulary were in the extremely low range; note that IQ and

adaptive behavior scores included in this report have a population mean of 100, standard deviation of 15. On the Wechsler Adult Intelligence Scale-Fourth Edition (WAIS-IV), she had a perceptual reasoning index score of 60 and a processing speed index score of 59. The decline from her prior full scale IQ measurement most likely reflects a deceleration in cognitive growth compared to same age peers rather than neurodegeneration. Further evaluation, conducted approximately one-year later, revealed an estimated Performance IQ in the extremely low range (WASI-II PIQ=53), as well as WRAT-4 word reading, spelling, and math computation in the extremely low range (SSs=55). These findings, as well as very low adaptive functioning based on Vineland Adaptive Behavior Scales (Vineland-II) parental report (composite score=54), suggests intellectual disability in the moderate range.

The younger affected sibling (Patient 2) was 18 years of age. Her expressive speech was more severely impaired than her sister's. She had delayed motor development and began walking at 5 years of age. Although she did not present with spasticity, she walked on her toes was suspected to have tight heel cords, thus requiring tendon release surgery at 4 years of age. On examination, she communicated mostly with signs. Head circumference was 54.5 cm (57th centile), height 148.1 cm (1st centile, -2SD), weight 45 kg (3rd centile). She had upward slanting of the palpebral fissures, prominent lateral eyebrows and mild prognathism. Her neurological examination was notable for absent speech, though she was able to follow commands. She showed signs of dysmetria and dysdiadochokinesia in her upper and lower extremities. Her gait was mildly wide-based. As for her sister, her brain MRI showed a MTS (Figure 1B, left panel).

On ocular examination, she had rotatory nystagmus, ocular motor apraxia, myopic astigmatism and retinal degeneration (Figure 1B), which was more advanced than her sister, and showed secondary optic atrophy. Best corrected visual acuity stood at logMAR 0.50 in the right eye and 0.60 in the left eye. ERG responses were delayed, with amplitudes at 30% of the lower limit of normal for both photopic and scotopic responses.

The auditory brainstem response of Patient 2 was abnormal, similar to that of her older sister. On neuropsychological evaluation, she scored an adaptive behavior composite of 51 on her Vineland-II, which is in the moderately impaired range. Her Performance IQ from the Wechsler Abbreviated Scale of Intelligence (WASI) was 46, which combined with the estimate of adaptive functioning, indicates intellectual disability in the moderate range of severity. Subtests from the Leiter International Performance Scale, a non-verbal measure of cognitive function yielded similar estimate.

In both patients, abdominal ultrasonography with Doppler, liver function tests, renal function tests and urinalysis were generally normal, making congenital hepatic fibrosis and nephronophthisis unlikely. Abdominal MRI for Patient 2 showed a 5 mm cyst within the medial lower pole of the right kidney, but kidney function tests and blood pressure were normal.

Molecular Data and Analysis of Cilia in Fibroblasts

A clinical chromosomal microarray revealed previously unknown consanguinity; the parents came from the same small region of Mexico. From the SNP-chip array, we obtained a list of

all areas of homozygosity shared between the proband and her affected sibling. These areas of shared homozygosity were then imported into the Miami ROH tool (see URLs). Four known genes that cause Joubert syndrome were located within the shared areas of homozygosity, including *INPP5E* (Supplementary Table 1), *CEP290*, *NHPI*, and *C20orf42*. Subsequent exome analysis confirmed a homozygous recessive variant in *INPP5E* (NM_019892.4:c.1565G>C; p.Gly522Ala; rs771866500) in the proband and the affected sibling, for which both parents are heterozygous carriers (Figure 1C). The disease segregating variant c.1565G>C has a Complete Annotation Dependent Depletion (CADD) (see URLs) Phred-scaled score of 26.40 and was ranked highest by Exomiser [Bone et al., 2015], with a combined score of 0.959. The c.1565G>C variant is known in ExAC, with 3 heterozygous individuals identified in the Latino population (minor allele frequency: 0.0002677 in Latino population, 0.0000253743 in total). This variant is predicted to be “Probably Damaging” (HumVar score: 0.979) by PolyPhen-2 (see URLs), “Deleterious” (Score: 0.03) by SIFT (see URLs) and Disease causing (p-value: 1) by MutationTaster (see URLs). Gly522 is highly conserved and is present in all vertebrates.

Expression of *INPP5E* mRNA transcript NM_019892.4 was increased fibroblasts of the affected individuals compared to control cells (Figure 2A), whereas western blot analysis (n=3) revealed a two-fold decrease in the amount of *INPP5E* protein relative to TUBA4A, compared to control fibroblasts (Figure 2B).

Imaging of the cilia revealed a clear qualitative and morphological difference between control and patient cells’ cilia (Figure 2C). Cilia appearing after 48 hours of serum starvation were 61% and 46% shorter in length in Patients 1 and 2, respectively, compared with control (Figure 2D); both patients displayed fewer ciliated fibroblasts than the control line (Figure 2E), although there was no statistical difference.

DISCUSSION

We identified a novel homozygous mutation in *INPP5E* in two sisters presenting with JS based on clinical phenotype and neuroradiological features, emphasizing the importance of correlating the clinical and radiologic findings with data gathered from next generation sequencing for accurate molecular diagnosis. Four candidate genes linked to JS were positioned within the regions of shared homozygosity; a combination of whole exome sequencing and variant segregation by Sanger sequencing confirmed that both affected siblings had *INPP5E* mutations. The 27 known *INPP5E* mutations, which are mostly missense and are scattered in the catalytic domain of the protein, lead to phenotypes of pure JS and JS with ocular involvement (Supplementary Figure 1 and Supplementary Table 2); these mutations are responsible for approximately 2.7% of all Joubert cases [Travaglini et al., 2013]. Mutations affecting the binding pocket phosphatase domain have been shown to impair 5-phosphatase activity and result in altered cellular phosphatidylinositol ratios, but neither missense nor nonsense mutations in the domain reduce the activity completely [Bielas et al., 2009; Conduit et al., 2012]. Interestingly, mutations in *INPP5E* have also been identified in mental retardation, truncal obesity, retinal dystrophy, and micropenis (MORM) syndrome [Jacoby et al., 2009], which can be distinguished from Bardet-Biedl syndrome and Cohen syndrome due to the nonprogressive nature of visual impairment.

Our patients' mutation is located in the *INPP5E* catalytic domain but because our mutation is missense we do not anticipate complete loss of enzyme activity. Our patients' phenotype included mainly neurological and ocular involvement without evidence for kidney or liver disease consistent with prior reports of rare renal or hepatic involvement in patients with *INPP5E* mutations (Supplementary Table 2). Still, it would be prudent to watch out for clinical signs of renal involvement, as four patients have been reported to have bilateral increased renal echogenicity with cysts or ectopia (Supplementary table 2). Similarly, a routine examination of the liver may be helpful, as two patients were documented to have elevated transaminase levels and fibrosis (Supplementary table 2). In terms of neurological symptoms, however, our patients seem to expand the clinical phenotype associated with *INPP5E*-related JS, as they exhibited more pronounced cerebellar signs, in addition to abnormalities recorded in evaluating auditory evoked potentials. Of note, both patients in this report have short stature, microsomia, and abnormal auditory brainstem response; whether this finding is specific to our patients in this report or included as one of the phenotypes associated with JS associated with *INPP5E* variants remains to be clarified. The possibility of having another genetic disorder, or a gene modifier, that could explain the occurrence of such symptoms, can only be addressed by future studies.

The *INPP5E* mutation in our patients may lead to the formation of an unstable protein, as supported by our biochemical data showing reduced levels of *INPP5E* in patients' fibroblasts, leading to impaired cilia formation. Indeed, the cilia present after 48 hours of serum starvation were shorter in both patients, and there were fewer total ciliated fibroblasts. The patients studied here have a missense *INPP5E* mutation and abnormal cilia length and number, highlighting the importance of *INPP5E* not only in cilia maintenance [Bielas et al., 2009], but also in ciliogenesis [Xu et al., 2016a; Xu et al., 2016b]. Our findings are supported by studies using animal models. Mice that lack *Inpp5e* are embryonic lethal; homozygous mice at E18.5 show several features of ciliopathies and in addition, show reduced cilia numbers and abnormal morphology in kidney tubules and Bowman's capsule [Jacoby et al., 2009]. Recently, *INPP5E* has been shown to coordinate with a centrosomal PtdIns(4)P 5-kinase, PIPKI γ , highlighting the importance of *INPP5E* in the initiation of ciliogenesis [Xu et al., 2016a]. Our results are supported by recent studies showing defective ciliogenesis in *inpp5e* zebrafish morphants, which is reversed by PtdIns(3,4,5)P₃ inhibition [Xu et al., 2017]. In neural stem cells, *INPP5E* has been shown to regulate phosphoinositides; loss of *INPP5E* activity leads to accumulation of TULP3 (a protein required to traffic a subset of GPCRs to the cilium) and Gpr161, which ultimately lead to subsequent repression of Shh response [Chavez et al., 2015]. Future studies on Shh signaling pathways using fibroblasts from patients and controls will certainly contribute to the clarification of *INPP5E* function in regulating phosphoinositides.

The mid-hindbrain abnormalities observed in JS are considered to be a product of abnormalities in cell migration, as a result of the reduced functionality of the affected cilia [Doherty 2009]. Vermis hypoplasia in JS patients is considered to be a result of reduced proliferation and migration of germinal zone granule cell precursors, which later develop into granule neurons that do not align in a typical manner due to variations in signaling. While it is hypothesized that *INPP5E* defects can lead to aberrant cellular migration patterns during neonatal development, and some growth factors and morphogens in this altered this

pathway have been identified, further studies will be necessary to elucidate the pathogenic mechanism linking cell migration to the disease morphology of JS patients [Valente et al., 2014]. Recent studies have identified further clues on the function of INPP5E, including regulation of lysosomal phosphoinositide balance for autophagosome-lysosome fusion [Hasegawa et al., 2016; Nakamura et al., 2016], and defects in kidney PI3K/Akt/mTORC1 signaling [Hakim et al., 2016]. Identification of other patients with INPP5E mutations will help us understand genotype and phenotype correlation and contribute to study design for future therapies.

Supplementary Material

Refer to Web version on PubMed Central for supplementary material.

Acknowledgments

The authors do not have any conflict of interest to declare. We thank the patients and their parents for their participation in this study. This work was supported by the Intramural Research Program of the National Human Genome Research Institute and the Common Fund of the NIH Office of the Director. Barbara Pusey and the bioinformatics team at the NIH-UDP, specifically Trevor Frisby and Christopher Adams, provided computational information. We also thank Megan Kane for her mentorship and critical comments on our manuscript.

References

- Bielas SL, Silhavy JL, Brancati F, Kisseleva MV, Al-Gazali L, Sztriha L, Bayoumi RA, Zaki MS, Abdel-Aleem A, Rosti RO, Kayserili H, Swistun D, Scott LC, Bertini E, Boltshauser E, Fazzi E, Travaglini L, Field SJ, Gayral S, Jacoby M, Schurmans S, Dallapiccola B, Majerus PW, Valente EM, Gleeson JG. Mutations in INPP5E, encoding inositol polyphosphate-5-phosphatase E, link phosphatidyl inositol signaling to the ciliopathies. *Nat Genet.* 2009; 41(9):1032–1036. [PubMed: 19668216]
- Brancati F, Dallapiccola B, Valente EM. Joubert Syndrome and related disorders. *Orphanet journal of rare diseases.* 2010; 5:20. [PubMed: 20615230]
- Chavez M, Ena S, Van Sande J, de Kerchove d'Exaerde A, Schurmans S, Schiffmann SN. Modulation of Ciliary Phosphoinositide Content Regulates Trafficking and Sonic Hedgehog Signaling Output. *Dev Cell.* 2015; 34(3):338–350. [PubMed: 26190144]
- Conduit SE, Dyson JM, Mitchell CA. Inositol polyphosphate 5-phosphatases; new players in the regulation of cilia and ciliopathies. *FEBS letters.* 2012; 586(18):2846–2857. [PubMed: 22828281]
- de Goede C, Yue WW, Yan G, Ariyaratnam S, Chandler KE, Downes L, Khan N, Mohan M, Lowe M, Banka S. Role of reverse phenotyping in interpretation of next generation sequencing data and a review of INPP5E related disorders. *European journal of paediatric neurology : EJPN : official journal of the European Paediatric Neurology Society.* 2016; 20(2):286–295. [PubMed: 26748598]
- Doherty D. Joubert syndrome: insights into brain development, cilium biology, and complex disease. *Semin Pediatr Neurol.* 2009; 16(3):143–154. [PubMed: 19778711]
- Hakim S, Dyson JM, Feeney SJ, Davies EM, Sriratana A, Koenig MN, Plotnikova OV, Smyth IM, Ricardo SD, Hobbs RM, Mitchell CA. Inpp5e suppresses polycystic kidney disease via inhibition of PI3K/Akt-dependent mTORC1 signaling. *Human molecular genetics.* 2016; 25(11):2295–2313. [PubMed: 27056978]
- Hasegawa J, Iwamoto R, Otomo T, Nezu A, Hamasaki M, Yoshimori T. Autophagosome-lysosome fusion in neurons requires INPP5E, a protein associated with Joubert syndrome. *The EMBO journal.* 2016; 35(17):1853–1867. [PubMed: 27340123]
- Jacoby M, Cox JJ, Gayral S, Hampshire DJ, Ayub M, Blockmans M, Pernot E, Kisseleva MV, Compere P, Schiffmann SN, Gergely F, Riley JH, Perez-Morga D, Woods CG, Schurmans S. INPP5E mutations cause primary cilium signaling defects, ciliary instability and ciliopathies in human and mouse. *Nat Genet.* 2009; 41(9):1027–1031. [PubMed: 19668215]

- Malicdan MCV, Vilboux T, Stephen J, Maglic D, Mian L, Konzman D, Guo J, Yildirimli D, Bryant J, Fischer R, Zein WM, Snow J, Vemulapalli M, Mullikin JC, Toro C, Solomon BD, Niederhuber JE, Program NCS, Gahl WA, Gunay-Aygun M. Mutations in human homologue of chicken talpid3 gene (KIAA0586) cause a hybrid ciliopathy with overlapping features of Jeune and Joubert syndromes. *J Med Genet.* 2015; 52(12):830–839. [PubMed: 26386044]
- Nakamura S, Hasegawa J, Yoshimori T. Regulation of lysosomal phosphoinositide balance by INPP5E is essential for autophagosome-lysosome fusion. *Autophagy.* 2016:1–2. [PubMed: 26799652]
- Travaglini L, Brancati F, Silhavy J, Iannicelli M, Nickerson E, Elkhartoufi N, Scott E, Spencer E, Gabriel S, Thomas S, Ben-Zeev B, Bertini E, Boltshauser E, Chaouch M, Cilio MR, de Jong MM, Kayserili H, Ogur G, Poretti A, Signorini S, Uziel G, Zaki MS, International JSG, Johnson C, Attie-Bitach T, Gleeson JG, Valente EM, Ali Pacha L, Zankl A, Leventer R, Grattan-Smith P, Janecke A, Koch J, Freilinger M, D'Hooghe M, Sznajder Y, Vilain C, Van Coster R, Demerleir L, Dias K, Moco C, Moreira A, Ae Kim C, Maegawa G, Dakovic I, Loncarevic D, Mejaski-Bosnjak V, Petkovic D, Abdel-Salam GMH, Abdel-Aleem A, Marti I, Pinard JM, Quijano-Roy S, Sigaudy S, de Lonlay P, Romano S, Verloes A, Touraine R, Koenig M, Dollfus H, Flori E, Fradin M, Lagier-Tourenne C, Messer J, Collignon P, Penzien JM, Bussmann C, Merckenschlager A, Philippi H, Kurlmann G, Grundmann K, Dacou-Voutetakis C, Kitsiou Tzeli S, Pons R, Jerney J, Halldorsson S, Johannsdottir J, Ludvigsson P, Phadke SR, Girisha KM, Doshi H, Udani V, Kaul M, Stuart B, Magee A, Spiegel R, Shalev S, Mandel H, Lev D, Michelson M, Idit M, Ben-Zeev B, Gershoni-Baruch R, Ficcadenti A, Fischetto R, Gentile M, Della Monica M, Pezzani M, Graziano C, Seri M, Benedicenti F, Stanzial F, Borgatti R, Romaniello R, Accorsi P, Battaglia S, Fazzi E, Giordano L, Pinelli L, Boccone L, Barone R, Sorge G, Briatore E, Bigoni S, Ferlini A, Donati MA, Biancheri R, Caridi G, Divizia MT, Faravelli F, Ghiggeri G, Mirabelli M, Pessagno A, Rossi A, Uliana V, Amorini M, Briguglio M, Briuglia S, Salpietro CD, Tortorella G, Adami A, Bonati MT, Castorina P, D'Arrigo S, Lalatta F, Marra G, Moroni I, Pantaleoni C, Riva D, Scelsa B, Spaccini L, Del Giudice E, Ludwig K, Permunian A, Suppiej A, Macaluso C, Pichiecchio A, Battini R, Di Giacomo M, Priolo M, Timpani P, Pagani G, Di Sabato ML, Emma F, Leuzzi V, Mancini F, Majore S, Micalizzi A, Parisi P, Romani M, Stringini G, Zanni G, Ulgheri L, Pollazzon M, Renieri A, Belligni E, Grosso E, Pieri I, Silengo M, Devescovi R, Greco D, Romano C, Cazzagon M, Simonati A, Al-Tawari AA, Bastaki L, Megarbane A, Sabolic Avramovska V, Said E, Stromme P, Koul R, Rajab A, Azam M, Barbot C, Salih MA, Tabarki B, Jovic-Jakubi B, Martorell Sampol L, Rodriguez B, Pascual-Castroviejo I, Gener B, Puschmann A, Starck L, Capone A, Lemke J, Fluss J, Niedrist D, Hennekam RCM, Wolf N, Gouider-Khouja N, Kraoua I, Ceylaner S, Teber S, Akgul M, Anlar B, Comu S, Kayserili H, Yuksel A, Akcakus M, Caglayan AO, Aldemir O, Al Gazali L, Sztrihla L, Nicholl D, Woods CG, Bennett C, Hurst J, Sheridan E, Barnicoat A, Hemingway C, Lees M, Wakeling E, Blair E, Bernes S, Sanchez H, Clark AE, DeMarco E, Donahue C, Sherr E, Hahn J, Sanger TD, Gallager TE, Daugherty C, Krishnamoorthy KS, Sarco D, Walsh CA, McKanna T, Milisa J, Chung WK, De Vivo DC, Raynes H, Schubert R, Seward A, Brooks DG, Goldstein A, Caldwell J, Finsecke E, Maria BL, Holden K, Cruse RP, Karaca E, Swoboda KJ, Viskochil D, Dobyns WB. Phenotypic spectrum and prevalence of INPP5E mutations in Joubert syndrome and related disorders. *Eur J Hum Genet.* 2013; 21(10): 1074–1078. [PubMed: 23386033]
- Tsurusaki Y, Kobayashi Y, Hisano M, Ito S, Doi H, Nakashima M, Saito H, Matsumoto N, Miyake N. The diagnostic utility of exome sequencing in Joubert syndrome and related disorders. *Journal of human genetics.* 2013; 58(2):113–115. [PubMed: 23034536]
- Valente EM, Rosti RO, Gibbs E, Gleeson JG. Primary cilia in neurodevelopmental disorders. *Nat Rev Neurol.* 2014; 10(1):27–36. [PubMed: 24296655]
- Xu Q, Zhang Y, Wei Q, Huang Y, Hu J, Ling K. Phosphatidylinositol phosphate kinase PIPK γ and phosphatase INPP5E coordinate initiation of ciliogenesis. *Nat Commun.* 2016a; 7:10777. [PubMed: 26916822]
- Xu W, Jin M, Hu R, Wang H, Zhang F, Yuan S, Cao Y. The Joubert Syndrome Protein Inpp5e Controls Ciliogenesis by Regulating Phosphoinositides at the Apical Membrane. *Journal of the American Society of Nephrology : JASN.* 2016b
- Xu WY, Jin MM, Hu RK, Wang H, Zhang F, Yuan SL, Cao Y. The Joubert Syndrome Protein Inpp5e Controls Ciliogenesis by Regulating Phosphoinositides at the Apical Membrane. *Journal of the American Society of Nephrology.* 2017; 28(1):118–129. [PubMed: 27401686]

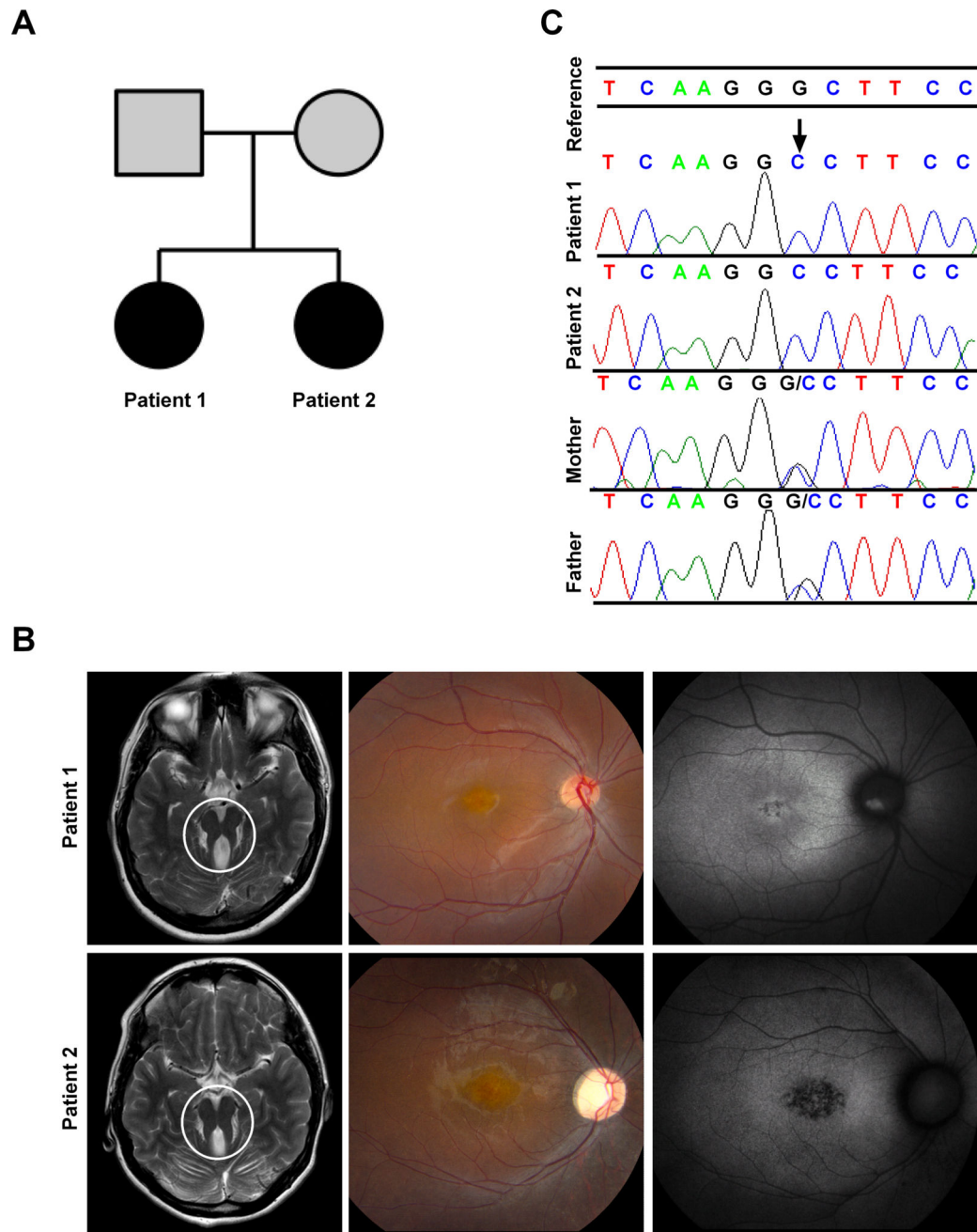


Figure 1. Clinical and Genetic Findings

(A) Pedigree of the family; affected members are shaded with black. (B) Left panel are MRI images showing the characteristic molar tooth sign (area encircled) in both Patient 1 and Patient 2. (C) Color fundus photography (middle panel) and fundus autofluorescence (right panel) of the right eye of Patient 1 and Patient 2. In Patient 1, color image shows macular pigmentary changes and mild vascular attenuation; fundus autofluorescence shows hypoautofluorescence centrally with a hyperautofluorescent area on the optic nerve head representing optic nerve head drusen. In Patient 2, color image shows macular pigmentary changes, moderate vascular attenuation, and waxy optic nerve head pallor; fundus

autofluorescence shows central hypoautofluorescence indicating retinal pigment epithelium atrophy with a hyperautofluorescent-surrounding ring (a common finding in retinal dystrophies).

(C) Chromatograms confirming the homozygous mutation at INPP5E c.1565G>C in the patients, and heterozygous mutations in the parents.

Author Manuscript

Author Manuscript

Author Manuscript

Author Manuscript

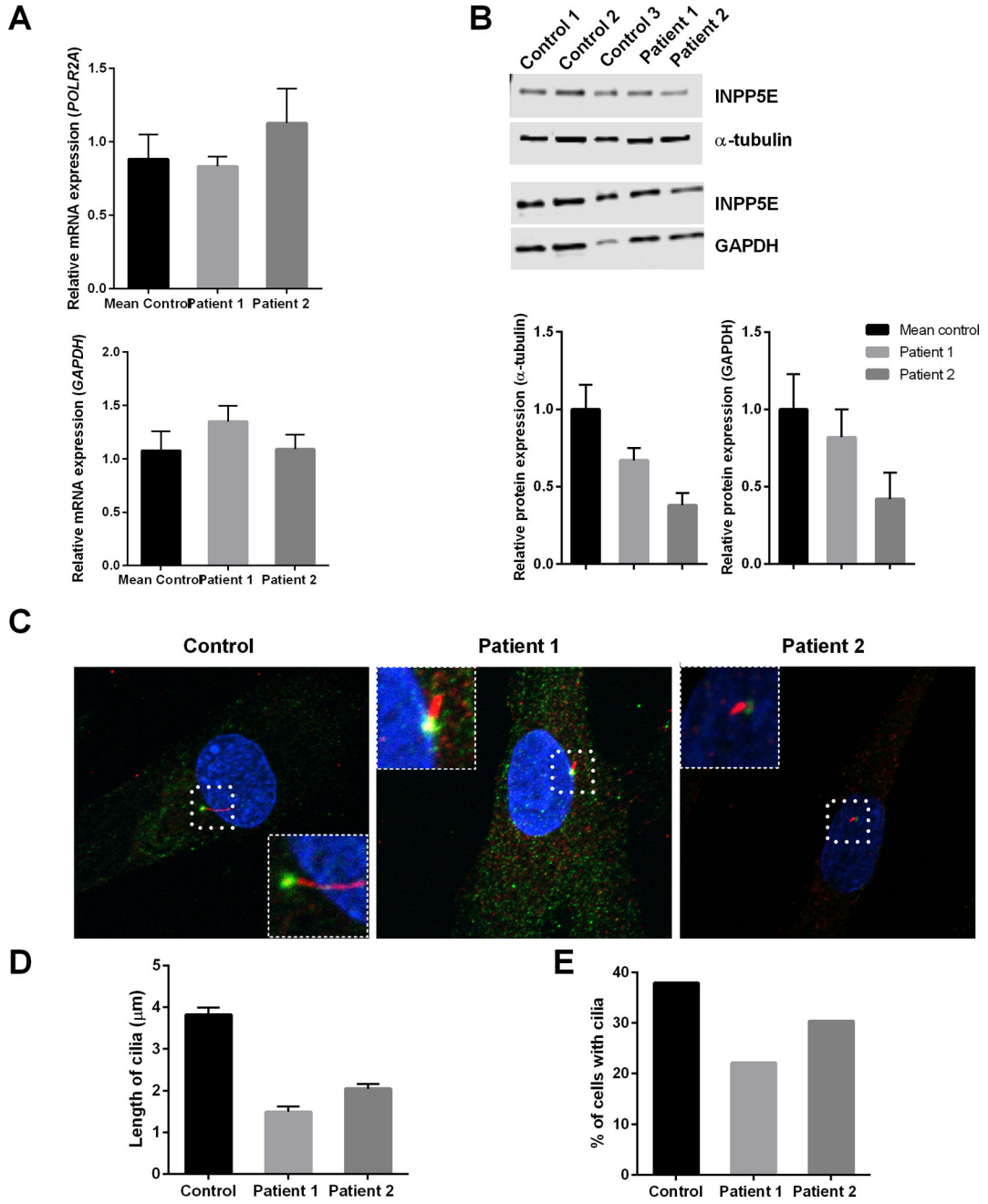


Figure 2. Molecular data and analysis of cilia in fibroblasts
 mRNA and western blot analyses show altered fibroblast INPP5E expression in the patients relative to control subjects (n=5). (A) *INPP5E* mRNA expression was normalized to *GAPDH* and *POLR2A*. (B) protein expression (66kDa) was normalized to α -tubulin (TUBA4A, 50 kDa) and *GAPDH* (37 kDa). (C) Representative cilia Control, Patient 1, and Patient 2. Cilia in cells is magnified and is shown in inset (D) Quantification of cilia length in fibroblasts after 48 hours of serum withdrawal. Error bars represent standard error. A total of greater than 200 cells were analyzed per replicate (four replicates). (E) Analysis of the

percentage of cells with cilia. A total of greater than 200 cells were analyzed per replicate (four replicates)

Author Manuscript

Author Manuscript

Author Manuscript

Author Manuscript

Table 1

Summary of neurological findings in patients with INPP5E-related JS

Clinical Features	Patient 1 (this study)	Patient 2 (this study)	[Bielas et al., 2009]	[Tsurusaki et al., 2013]	[Travaglini et al., 2013]	[de Goede et al., 2016]
Molar tooth sign on MRI	+	+	+	+	+	+
Cerebellar vermis hypoplasia	+	+	+	+	+	+
Global developmental delay	+	+	+	+	+	+
Intellectual disability	+	+	+	+	+	+
Language delay	+	+	NR	?	NR	+
Speech apraxia	+	+	+	?	NR	+
Intention tremor	+	+	NR	-	NR	+
Dysarthria	+	+	NR	NR	NR	NR
Thoracolumbar scoliosis	+	+	NR	NR	NR	NR
Neonatal breathing dysregulation	-	-	1 in 18 affected individuals	NR	7 in 17 affected individuals	NR
Proptosis	+	+	NR	+	1 in 17 affected individuals	-
Ocular motor apraxia	+	+	+	NR	+	+
Nystagmus	+	+	NR	+	NR	-
Retinal Degeneration	+	+	12 in 18 affected individuals	+	-	-
Short stature	+	+	NR	NR	NR	NR
Facial features	malar flattening, high-arched eyebrows, small earlobes, and mild prognathism	malar flattening high-arched eyebrows, small earlobes, and mild prognathism, upward slanting of palpebral feature		Frontal bossing, epicanthal fold	NR	Receding forehead, hypertelorism, and synophrys
Abnormal auditory evoked potentials	+	+		NR	NR	NR
Microsomnia	severe	-	NR	NR	NR	NR
Ataxia	Wide based-gait	Wide based-gait	+	NR	NR	NR
Dysmetria	+	+		NR	NR	NR
Dysdiadochokinesia	-	+		NR	NR	+

“+” denotes presence of a feature; “-” denotes absence of a feature; “NR” represents not reported.